

## Simulation of the metallographic structures in the heat affected zone of a welded joint

Pavel-Michel Almaguer-Zaldivar<sup>1</sup>, Julio-César Pino-Tarragó<sup>2</sup>

<sup>1</sup>(CAD/CAM Study Center, Faculty of Engineering/ University of Holguín, Cuba)

<sup>2</sup>((Civil Engineering Career, Faculty of Technical Sciences/ University of Manabí, Ecuador)

Corresponding Author; Pavel-Michel Almaguer-Zaldivar

---

**Abstract:** The results of the simulations by means of heat treatments of the different metallographic structures that takes place in a butt-welded joint of AISI 1015 steel and as contribution material the electrode E6013 Cuban manufacturing are exposed in the presently work. The heating parameters are determined by each zone between of heat affected zone and by means of the application of the method of finite elements the cooling speeds are obtained in each case. The results of the tensile test, metallographic observations and hardness and micro hardness test are also shown. As results it is obtained that likeness exist in the constituent elements of the simulated structures and those that take place in the welded joint, therefore, with the proposed model it is possible to carried out the simulation improving the process.

**Keywords** -AISI 1015 steel, finite elements method, heat affected zone, heat treatment, welded joint

---

Date of Submission: 02-06-2019

Date of acceptance: 18-06-2019

---

### I. INTRODUCTION

When the welded joint is made between two pieces of steel, a commonly used process is Shield Metal Arc Welding. In the joints obtained by this process, three zones are defined in the welded joint: filler material (FM), heat affected zone (HAZ) and base material (BM).

The HAZ is the part of the base metal that does not melt, but due to the high temperature reached during the welding process, it undergoes changes in its structure that cause the variation of its mechanical properties. The distribution of the temperature in this zone always decreases from the center of the weld bead to the parts of the base metal that remain cold.

In the HAZ, depending on the maximum temperature reached and the cooling speed, a different heat treatment is produced at each point of the same. That is why the heat affected zone is divided into three fundamental parts, according to three main isotherms. In the case of steels these three zones are known as: [1]

- Overheating zone: it is located between the boundary of the melted zone with the base metal (called the transition zone) and the isotherm of 1 100 °C.
- Annealing zone: defined between the isotherm of 1 100 °C and 900 °C.
- Zone of the first transformation: located between the isotherm of 900 °C and that of 700 °C.

After the isotherm of 700 °C, the base metal is heated without occur thermal affectation.

Analyzing these characteristics, it is possible to consider the modeling of each one of the structures that are formed in the HAZ as if it were a homogeneous material.

Numerous researchers have studied the characteristics of the HAZ. Such is the case of Reina [2] who studied the qualitative variation of ultimate loads and toughness as a function of the temperatures reached in the HAZ and in the BM in the welding of a normalized steel. Within the HAZ there is an appreciable growth of the grain in the zone adjacent to the melting line. These metallographic structures cause residual stresses to arise, which when acting in load mode I favor the growth of cracks.

In his doctoral thesis, Cheng [3] studied the heterogeneity of the different areas of the HAZ by heat treatments. He used tubular specimens heated at different temperatures. The Young modulus of all specimens was similar, however the yield limit and the ultimate stresses decreased with the increase in temperature at which the different specimens were treated.

In another work [4] the simulation of the HAZ of an API X-70 steel welded with a laser welding process was carried out by heat treatments. It was determined that there were similarities between the metallographic structures that were formed in the heat-treated and welded specimen.

Other researchers have also studied the effect of post-weld heat treatment (PWHT) on the mechanical properties of welded joints. The effect of the tempering pass technique (TWB) and the PWHT on multiple-pass welded joints where the BM was a low-carbon steel was studied in another investigation [5]. The yield limit and the tensile strength, with both treatments achieved acceptable results, however, with the TWB the values

reached were closer to those of the MB. In another work [6] the effect of PWHT on a high strength steel was studied. The results showed that in the joint the mechanical properties greater than the minimum values required for the welds of the steel studied. The microstructure due to PWHT in a BA-160 steel was studied by Yue et al. [7] It was found that with a PWHT of 650 °C for one hour the improvement of the resistance in the coarse-grained zone of the HAZ was obtained. The changes in the resistance that occur with the PWHT in the welded joint, are related to the microstructure that can be achieved with the thermal treatment.

The authors Liu et al. [8] simulated and studied the microstructure and properties of the HAZ of welded joints of one and two passes. For this they used a Gleeble 3500-HS thermal-mechanical simulation machine. They obtained that in the coarse grain zone the increase in hardness is significant when small values of added heat were used. The analyzes carried out allowed to optimize the measurements of the microstructure and properties of X100 steel pipes.

The thermal simulation of the HAZ is a fast and economical process to evaluate the phase transformations in the steels that are subjected to thermal cycles during the welding process, as well as to obtain the diagrams. [9] Kong [10] used a GLEEBLE 3800 thermal simulation machine to study the effect of different chemical elements on the impact properties on the X80 steel joints. It was obtained that the best impact toughness was achieved with the higher nickel, molybdenum and chromium content.

Kulhánek et al. [11] simulated thermal cycles in standardized specimens. The microstructure and hardness were identical to those obtained in welded joints. For this they developed a simulator of temperature cycles with a vacuum chamber. The results presented by these authors demonstrated the possibility of using thermal simulation to obtain specimens that allow the evaluation of the HAZ.

The thermal simulation was used by Węglowski [12] to study the effect of t8/5 on the microstructure and mechanical properties in the HAZ of a Weldox 1300 steel. It was obtained that the impact toughness and hardness decreased with the increase in t8/5.

Moon et al. [13] simulated the HAZ with a Gleeble simulator. The susceptibility to cracking due to overheating increased with the increase of the temperatures in the post-weld heat treatment.

Several authors to carry out the study of welded joints have used the numerical simulation. The possibility offered by the finite elements of simulating thermal processes is presented as an interesting option for the evaluation of the phenomena that take place in welded joints. Numerous authors have used this method and the results obtained have demonstrated the feasibility of numerical methods to study welds that were similar. In this way the feasibility of the simulation to select the parameters of the welding process was demonstrated.

As has been appreciated so far, thermal treatments are presented as a good option to perform the study of welded joints, as welding is a process where high temperatures are reached that cause structural changes, and therefore, in the mechanical properties of the materials used for the manufacture of the union. At the same time, simulation techniques using the finite element method are also a tool to understand the different and complex processes that occur during soldering.

The objective of this work is to show the results of a study carried out using AISI 1015 steel to simulate by heat treatments the HAZ of a welded joint. Different mechanical tests were carried out to determine different mechanical properties. The cooling rate was obtained by the finite element method.

## II. MATERIALS AND METHODS

The mechanical characterization of the joints has the problem of metallurgical differences between the different zones in the joint. This is the importance of finding solutions to characterize them, mainly in the HAZ, where due to its small dimensions it is practically impossible to obtain conventional specimens.

In this work a structural steel AISI 1015 is used to simulate by means of heat treatments the HAZ of a butt welded joint, built with a Shield Metal Arc Welding process, with a current intensity and a voltage equal to 100 A and 25 V, respectively. The thickness of the sheet was 4 mm. The metallographic structure obtained in this way is compared with the structure present in a welded joint studied in previous research. [14, 15] The chemical composition and mechanical properties of the steel studied are shown in Table 1.

**Table 1.** AISI 1015 steel Chemical composition and physical – mechanical properties. [16]

Parameter	Value	Unit
Carbon (C)	0,13-0,18	%
Manganese (Mn)	0,3- 0,6	%
Iron (Fe)	99,13– 99,57	%
Sulphur (S)	0,05	%
Phosphorous (P)	0,04	%
Ultimate stress ( $\sigma_r$ )	430	MPa
Yield limit ( $\sigma_y$ )	315	MPa
Poisson's coefficient ( $\mu$ )	0,29	
Density ( $\rho$ )	7870	kg/m <sup>3</sup>
Thermal dilatation coefficient ( $\alpha$ )	119,10 <sup>-7</sup>	1/°C

Elongation ( $\delta$ )	39	%
Reduction of Area ( $\psi$ )	61	%
Hardness	71	HRB

### 1.2. Simulation by thermal treatments of the different structures that form in the HAZ due to the uneven heating of the BM.

The HAZ is the base metal part contiguous to the melted zone that does not melt, but where due to the complexity of the heat distribution during the welding process important metallurgical transformations take place. In this zone a variable thermal treatment takes place, due to which variations in the mechanical properties and in the metallurgical structure of the BM occur.

The study of the HAZ has an essential character, mainly in those steels sensitive to tempering, where due to the thermal cycles imposed on the joint metallurgical structures of high hardness and fragility are formed. The combination of these characteristics, with the thermal stresses caused by the heat added to the joint and those due to structural loads, often causes cracks in this zone.

The process of grain growth in steels depends on the temperature reached during heating and the permanencetime at that temperature. Since these are the essential parameters of the heat treatment, it can be said that it is possible to simulate the HAZ of the welded joint by means of heat treatment processes.

For a better approximation of the process, it is intended to perform heat treatments to different specimens at the temperatures defined by the isotherms explained above.

It is then proposed to perform the following heat treatments to simulate each zone:

1. Overheating zone: heat treatment at temperature  $T= 1\ 150\ ^\circ\text{C}$ .
2. Annealing zone: heat treatment at  $T= 950\ ^\circ\text{C}$ .
3. Zone of the first transformation: heat treatment at  $T= 750^\circ\text{C}$ .

The main objective of these tests is to determine the mechanical properties of each area of the HAZ. For this, tensile test specimens (Fig. 1) defined according to the standard NC 04-01: Tensile tests of metals; [17] that will be submitted to the heat treatments proposed and after the tensile test, obtaining the stress-strain curves of each specimen.

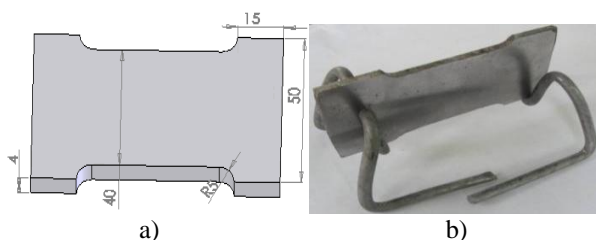


**Figure 1.** Specimens for the simulation by heat treatments of the different metallographic structures that are present in the welded joint. a) Isometric b) Specimen in the position that is inserted into the oven and devices designed to perform heat treatments.

In order to validate these experiments, the metallographic observations of each specimen will be made, to compare the results with the observations made to the HAZ of welded specimens.

The time that the heat treatment lasts is possible to decompose it in 3 times:

- 1)  $t_c$ : Warm up time to the temperature at which the specimen is to be treated.
- 2)  $t_p$ : Time of permanence of the specimen at the temperature to be treated.

The sum of both is the total warm-up time.

3)  $t_c$ : Cooling time; which is not normally calculated in the heat treatment processes. However, as in this research, it is intended to simulate the structure of the different HAZ zones and the cooling speed is an important parameter in the formation of these structures in the welded joint, if we calculate this time in order to determine the cooling speed. This will be done by simulating this process, using the thermal analysis module of the Simulation complement of the SolidWorks 2015 software. The procedure used will be detailed in the next paragraphs, when the results of the work are exposed.

The heating time depends on the ability of the medium to heat, the dimensions and geometrical configuration of the specimen and its placement into the oven, so it is possible to determine it from the following empirical formula (1): [18]

$$t_c = 0,1K_1K_2K_3 \quad (1)$$

Where:

D: is the dimensional characteristic of the piece, given in millimeters. The specimen selected for the study has a sheet form (Fig. 1), in this case the dimensional characteristic is the thickness, that is  $D= 4\ \text{mm}$ . Fig. 1b) shows the way in which the specimens are placed in the furnace.

$K_1$ : is the coefficient of the medium, as the piece will be tempered in a gaseous medium (air)  $K_1= 2$ .

$K_2$ : is the coefficient of form, for a sheet  $K_2= 4$ .

$K_3$ : is the coefficient of uniformity of the heating, this will be done everywhere so  $K_3= 1$ .

The result is obtained in minutes.

Substituting these values in (1), we obtain that  $t_c= 3.2$  min.

The permanence time  $t_p$  depends on the speed of the phase changes, which is determined by the degree of overheating above the critical point and by the dispersion of the initial structure. For AISI 1015 steel, in practice  $t_p$  can be taken equal to one minute. [18]

The cooling of the specimens was in the air using an axial fan; with the purpose of simulating as much as possible the structures that are formed in the heat affected zone of the joints made by the Shield Metal Arc Welding process that will be used to carry out the study in the specimens, where it happens that the parts to be joined they are subjected to high temperatures abruptly and then cooled in the air, however rapid cooling occurs. According to the temperature that reaches a certain zone of the HAZ, so will the internal structure and mechanical properties. As the cooling will be done in the air, the time is not considered in the calculation of the total heat treatment time.

Then the total thermal treatment time was determined by expression (2):

$$t_t = t_c + t_p \quad (2)$$

$t_t= 4,2$  min o 4 min y 12 s.

To perform the different heat treatments, the following sequence must be followed:

1. Heat the oven to 50 °C above the respective heating temperature.
2. After reaching the technological temperature, the piece is placed in the oven.
3. At the end of 4 minutes and 12 seconds the piece is removed.
4. Allow to cool in air, under the action of a fan until it reaches room temperature.

The oven used to perform the heat treatments is a TIP-241GAT model of Russian manufacture.

In order to carry out the heat treatments, guaranteeing the heating on all sides, in addition to preventing the specimens from copying possible defects of the surface where they were supported, a device was designed as shown in Figure 1b).

After carrying out the thermal treatments, the following experiments must be carried out:

1. Hardness test. It will allow to determine the surface hardness of the different structures that are formed with each one of the heat treatments. The comparison of the results obtained by means of this test, with the one carried out along the welded joint, will make it possible to judge the distribution of the different zones of the HAZ in the welded joint.
2. Tensile test. The aim is to determine the mechanical properties of each structure formed during the different heat treatment processes. The results obtained will be used later in the mechanical characterization.
3. Metallographic observation. To judge the similarity or not of the metallographic structures that are formed in the heat treated specimens and those formed in the HAZ of the welded joint.
4. Microhardness test. The microhardness chains, both in the heat treated and welded specimens, will be another way of evaluating the feasibility of simulating the HAZ of the welded joints by heat treatments.
5. Simulation of the cooling process. The aim is to determine the cooling speed.

### III. RESULTS

#### 3.1. Hardness test

Table 2 shows the measurements obtained from the surface hardness tests carried out on all the heat treated specimens. In each specimen, three measurements were made and then averaged to obtain the hardness of each sample. A Hoytom durometer, type Minor\*60, was used. The load was 100 kg and a steel ball with a diameter of 1/16 "was used as an indenter.

The following nomenclature was used to name each specimen: TT (means that it is a heat treated specimen), the two numbers that continue correspond to the number of the specimen, while the last three indicate the temperature to which they were heated.

**Table 2.** Surface hardness of the heat treated samples.

Specimen	Hardness (HRB)			Medium value (HRB)
TT01 750	73	74	74	73,67
TT02 950	71	72	71	71,33
TT03 950	75	74	72	73,67
TT04 1150	72	72,5	72	72,17
TT05 1150	71	72	72	71,67

The Fig. 2 is a comparison of the hardness of the surface layer of the different specimens and the welded joint.

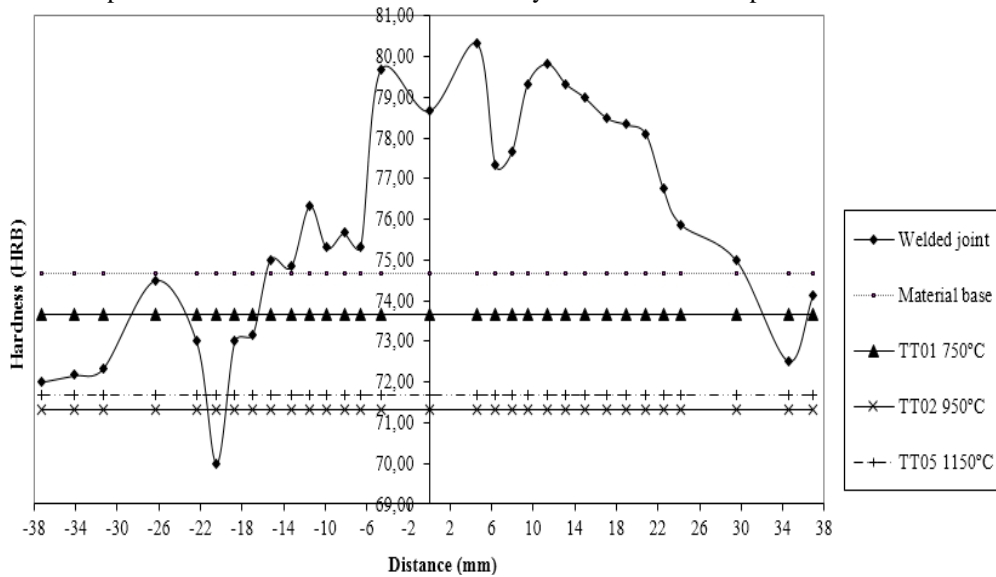


Figure 2. Comparison of the hardness of the heat treated specimens and the welded joint.

As seen in Fig. 2, the surface hardness values of the heat treated specimens do not correspond to the different zones that were simulated with them. The cause of this lies in the chemical composition of the base material used in this work. The low percentage of carbon makes the material susceptible to decarburization processes in thermal treatments, thus causing a decrease in surface hardness.

### 3.2. Tensile test.

The different test specimens were subjected to the conventional tensile test on an MTS 810 universal machine. Fig. 3 shows the stress - strain curves of the specimens heated at different temperatures.

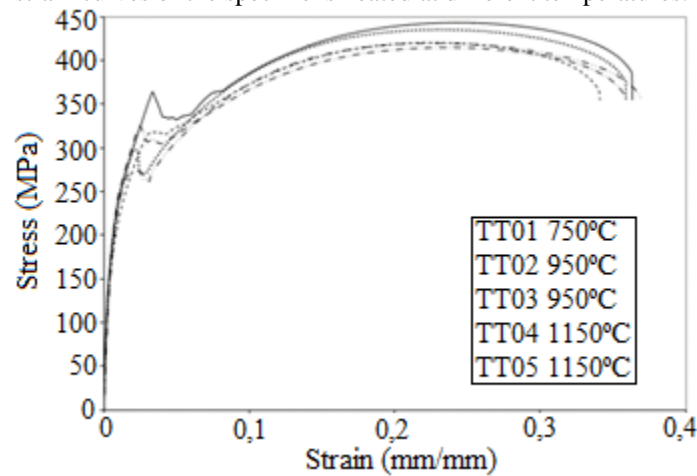


Figure 3. Stress - strain curve of the heated specimens.

The mechanical characteristics of the different specimens are expressed in Table 3.

Table 3. Parameters of the heat-treated specimens subjected to the tensile test.

Specimen	$\sigma_y$ (MPa)	$\sigma_r$ (MPa)	Plasticity	
			K	n
TT01 750	355	443	633,16	0,2076
TT02 950	317	415	584,94	0,1968
TT03 950	317	420	595,68	0,1977
TT04 1150	289	435	660,05	0,2276
TT05 1150	272	420	630,96	0,2204

As seen in Table 3, with the increase of the heat treatment temperature, there was a deterioration of the mechanical properties of the specimens, mainly in the yield limit where the reduction is significant, however the ultimate stress decreases very little. This highlights once again the difference in mechanical properties that

occurs between the different zones of the HAZ, due to the unequal distribution of temperatures during welding processes. The modulus of elasticity  $E$  practically does not vary and corresponds to the typical values for steels. On the other hand, the plasticity parameters  $K$  and  $n$  also vary very little, and as seen in Fig. 3 all the stress - strain curves have a similar behavior in the plastic zone. It continues to be shown that the greatest difference takes place in the yield stress.

### 3.3. Microhardness test.

Three measurements were made to each specimen, which were averaged to determine the microhardness at each level of the depth. The standard consulted for these tests was "ASTM E 384 - 99 Standard Test Method for Microindentation Hardness of Materials". [19] The load used was 10 g.

Below is a graph (Fig. 4) comparing the variation of the microhardness in the heat treated specimens and in the welded joint through the thickness of the specimens. For the former, the average microhardness values for each of them are represented by a horizontal line. In the case of the welded joint, each series of data represents the variation of the microhardness in the thickness of the sample. As indicated in the Fig. 4, the measurements are started by taking as a reference the section change between the melted zone and the heat affected zone. According to the observed values, it can be seen that in the zone near the beginning of the zone of coarse grains of the HAZ, approximately between 1 and 2 mm of the change of section, the microhardness chains tend to approach the line that represents the specimen treated at 1150 °C. This behavior is also observed at 3 mm, but this time the chains approach the representation of the sample TT02 950, while at distances close to 6 mm it happens that the measurements tend to the line of the sample TT01 750.

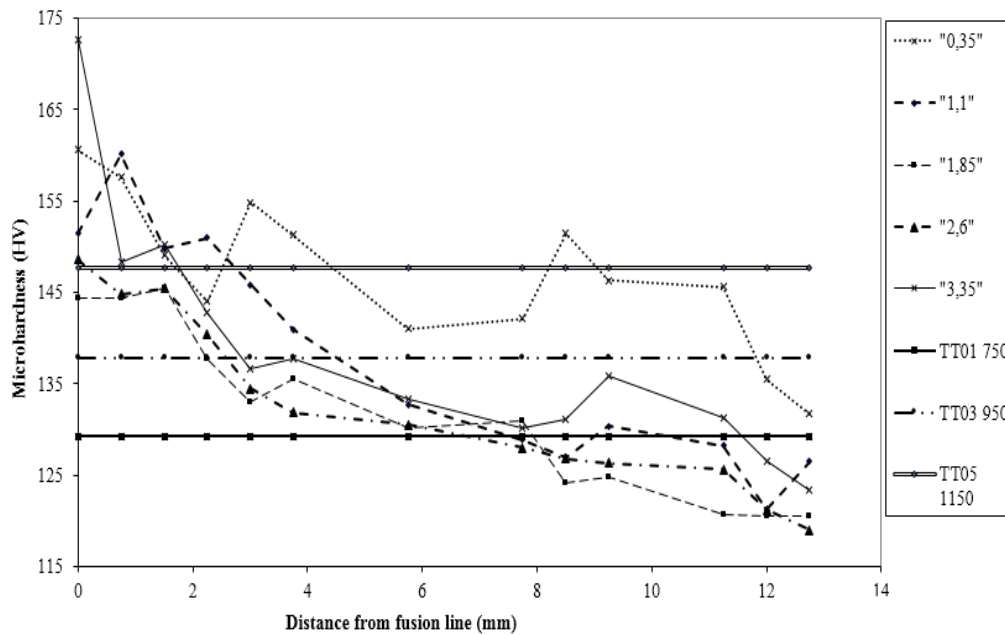
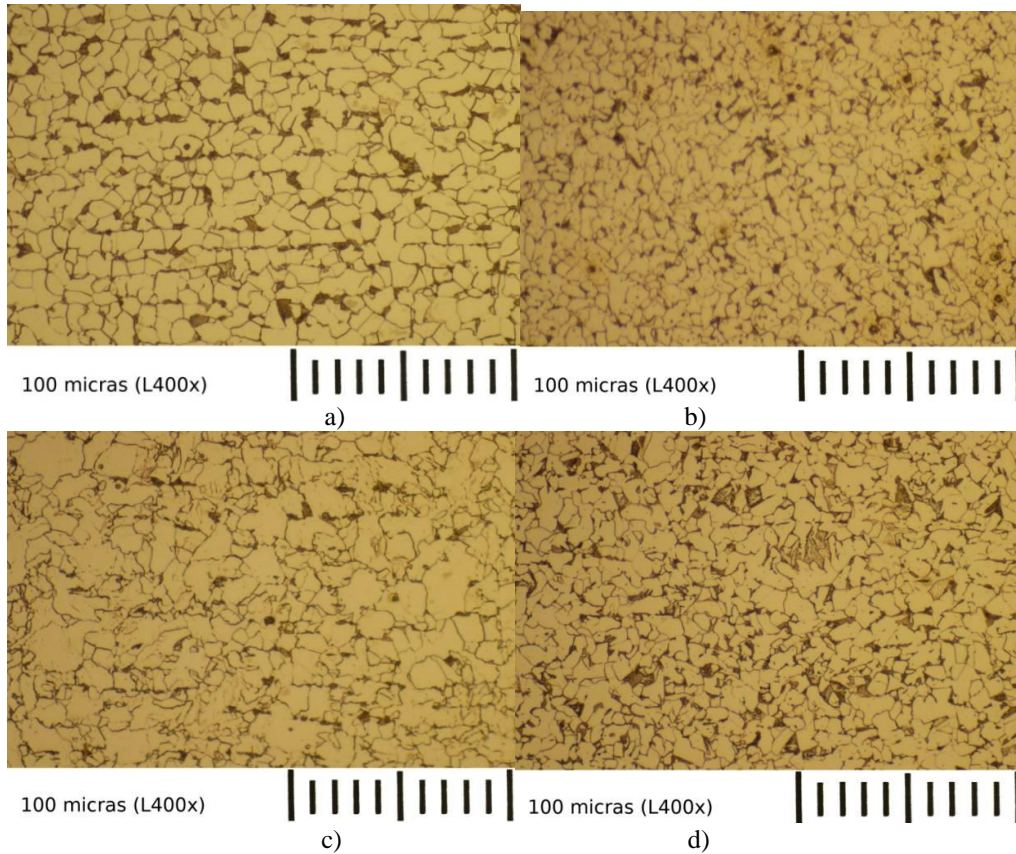


Figure 4. Microhardness profiles in the heat treated specimens and in the welded joint.

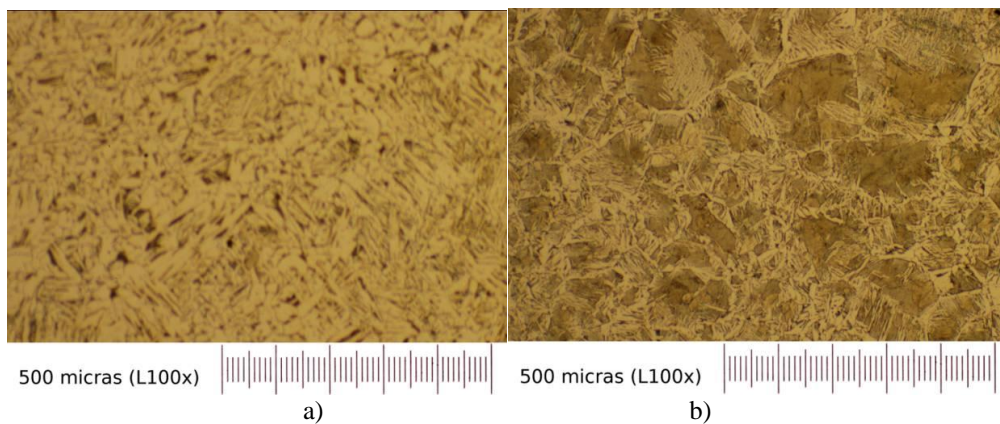
### 3.4. Metallographic observation.

The metallographic observation of the different heat treated specimens will allow, by comparing with the observations made in the different zones of the HAZ of a welded joint, to corroborate if there are similarities or not in the metallographic structures. In each of the following (Fig. 5 and 6) the images a) and c) show an observation of the heat treated specimen; while images b) and c) illustrate a similar area of the HAZ in the welded joint. Similarities are seen in the metallographic structures shown in the different images.



**Figure 5.** Metallographic structures: a) Specimen heated to 750°C. b) External area of the HAZ of the welded joint. c) Test piece heated to 950 ° C. d) Middle zone of the HAZ of the welded joint. 400x

In Fig. 6 a) and c) lengthened needles are seen which are also seen in Fig. 6 b) and d). These correspond to Widmanstaetten's structures. This one are a structure that is characterized by having great fragility, with needles that follow several directions. It usually occurs in the molten zone, although they also occur in the HAZ. It causes a small impact resistance, that is, it increases the fragility of the welded joint.



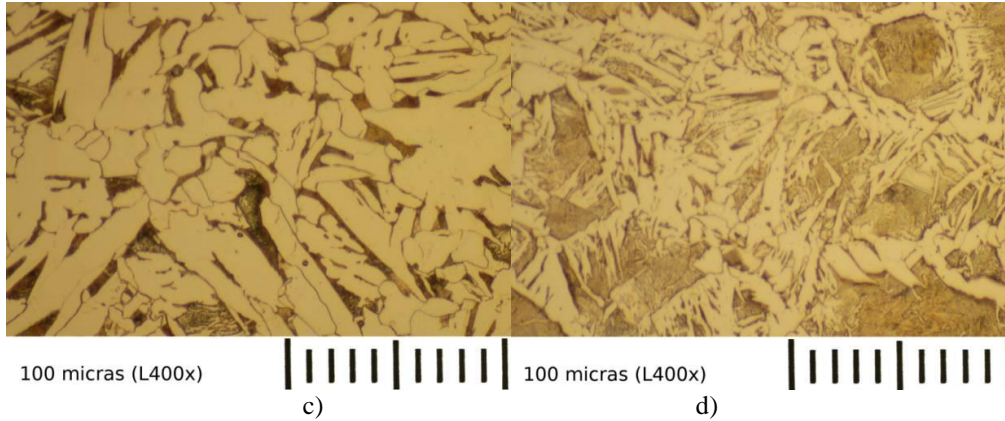


**Figure 6.** Metallographic structures: a) Specimen heated to 1150°C. b) Coarse-grained zone of the HAZ of the welded joint. 100x c) Specimen heated to 1150 °C. d) Coarse-grained zone of the HAZ of the welded joint. 400x

In the images of Fig. 6 c) and d) it is possible to observe similarities between the grain size of the coarse grain area simulated by thermal treatments and that which forms at the welded joint. Metallographic structures in the form of elongated needles corresponding to the structure of Widmanstaetten are also appreciated.

### 3.5. Cooling speed in the heat treatment.

An important parameter in the structure obtained in the different zones of the HAZ of the welded joint is the cooling speed  $v_c$ . Hence, its knowledge is of great importance in the simulation of the HAZ by heat treatments to achieve the greatest similarities between the metallographic structures that are formed due to the two processes.

In order to determine the cooling speed, in the different heat treatments carried out, the module for the thermal analysis incorporated in the SolidWorks 2015 software in the Simulation complement was used in this investigation. The geometric model used for the simulations will be the same as the actual specimen used to perform the heat treatments shown in Fig. 1.

In addition to the geometric model; other data necessary to perform the numerical simulations are the initial temperature  $T_0$ , the way in which the heat is dissipated and the heat transfer coefficient  $h$  that has units of measure Watt/(m°C).

To carry out the simulations, it is considered that the variation of the temperature in time is measured from the moment in which the test piece is extracted from the oven, therefore the initial temperature  $T_0$  will be the one defined for each of the three heat treatments that were made, and that were raised in point 2.1; that is, modeling will be carried out starting from 750 °C, 950 °C and 1150 °C.

Regarding the way in which the heat is dissipated, taking into account the sheet configuration of the specimens, in addition to the fact that they were located in a device (Fig. 1b) inside a forced air flow, it is concluded that forced convection exists over all the faces of the specimen. The effect of radiation and conduction between the specimen and the device is neglected due to the small area of exchange between them.

To determine the individual heat transfer coefficient, the theories of fluid mechanics and heat transfer are used.

Applying the equation of the flow of a fluid (3) it is possible to determine the speed that takes the air to the exit of the fan.

$$G = S_a v_a \quad (3)$$

Where:

G: It is the volume of air delivered by the fan. This value is obtained from the parameters that were observed in the plate of the equipment and is equal to 2900 m<sup>3</sup>/h.

S<sub>a</sub>: It is the cross section through which the flow circulates. It is defined as the area of the circumference defined by the diameter of the fan blades  $d_{alabes} = 54,5$  cm. This area is calculated according to (4):

$$S_a = \frac{\pi}{4} d_{alabes}^2 \quad (4)$$

S<sub>a</sub> = 0,2332 m<sup>2</sup>.

v<sub>a</sub>: Is the air velocity at the fan outlet. It is calculated by clearing it from the flow equation.



$$z_1 + \frac{p_1}{\gamma} + \frac{v_1^2}{2g} = z_2 + \frac{p_2}{\gamma} + \frac{v_2^2}{2g} + \sum h_{1-2} \quad (5)$$

Where:

The terms with subscript 1 correspond to the state of the fluid where the process begins to be studied (at the exit of the fan); while the subscript 2 indicates where the flow is stopped (next to the specimen).

$z_1, z_2$ : Height of fluid position (m). In this study they are the same.

$\gamma$ : Specific weight of the fluid ( $N/m^3$ ).

$g$ : Acceleration of gravity ( $9,81 \text{ m/s}^2$ ).

$p_1, p_2$ : Fluid pressure ( $N/m^2$ ).

$v_1, v_2$ : Speed of the fluid (m/s).

$\Sigma h_{1-2}$ : Losses of energy in the flow due to friction and turbulence in the accessories (m). The specimens were located 0,4 m from the fan impeller, so it is possible to neglect the losses due to friction and turbulence in the absence of intermediate accessories, as well as pressure variations, therefore we can consider that the speed with which arrives the air to the specimens is the same with the one that comes out of the fan (6), that is:

$$v_2 = v_1 = v_a = 3,455 \text{ m/s} \quad (6)$$

After calculating the air speed, the theory of heat transfer is applied, but first it is necessary to determine the Reynolds's Number (7), to know if the regime with which the air moves is turbulent or not. This dimensionless number is determined by the following expression:

$$Re_{\eta} = \frac{v_a L_0}{\nu} \quad (7)$$

$Re_{\eta}$ : is the Reynolds number determined at the fluid temperature and taking as reference magnitude the length of the plate, indicated by the subscripts f and l respectively. If its value is less than 2300, the air flow regime is laminar, while for higher values it is turbulent.

$L_0$ : is the reference dimension that influences the movement of the fluid. In this study it is taken as the length of the specimen.  $L_0 = 80 \text{ mm}$ .

$\nu$ : is the kinematic viscosity of the air at the flow temperature.

The properties of the air were determined at the room temperature that the heat treatments were carried out. The time and temperature at which the heat treatments were carried out are shown in Table 4. The physical properties of the flow must be determined at the temperature of the air. In the bibliography consulted [18] these properties are found at temperatures of 20 and 30 °C, so it is necessary to interpolate the known values to determine the properties at room temperatures. The Table 4 shows the results obtained:

**Table 4. Room temperature and physical properties of the air at the atmospheric temperature at which the thermal treatments were carried out. [20]**

Time	Room Temperature $T_a$ (°C)	Thermal conductivity $\lambda$ (W/(m°C))	Kinematic viscosity $\nu$ (m <sup>2</sup> /s)
-	20,0	$2,59 \times 10^{-2}$	$15,06 \times 10^{-6}$
10:00	23,9	$2,6212 \times 10^{-2}$	$15,4266 \times 10^{-6}$
13:00	24,3	$2,6244 \times 10^{-2}$	$15,4642 \times 10^{-6}$
16:00	26,7	$2,6436 \times 10^{-2}$	$15,6898 \times 10^{-6}$
-	30,0	$2,67 \times 10^{-2}$	$16,00 \times 10^{-6}$

For cooling from 750 °C:

$$Re_{\eta} = 17\ 916$$

For cooling from 950 °C:

$$Re_{\eta} = 17\ 616$$

For cooling from 1 150 °C:

$$Re_{\eta} = 17\ 873$$

Since all the values determined using expression (7) are greater than 2300, we are in the presence of a turbulent regime in each case.

According to the flow-test arrangement it is stated that it is a typical case of forced flow on a flat plate, where the individual coefficient is determined from the number of Nusselt calculated by the following expression (8):

$$Nu_{\eta} = 0,032 Re_{\eta}^{0,8} \quad (8)$$

$Nu_{\eta}$ : dimensionless Nusselt number, determined according to the same conditions as the Reynolds number.

In general, the Nusselt number is calculated from the following expression (9). In the same h is the individual coefficient of heat transfer (which is removed from (9)) and  $\lambda$  the thermal conductivity of the air.

$$Nu = \frac{h L_0}{\lambda} \quad (9)$$

Then:

For cooling from 750 °C:

$$Nu_{\eta} = 80,864$$

$$h = 26.495 \text{ W / m}^2$$

For cooling from 950 ° C:

$$Nu_{\eta} = 79,777$$

$$h = 26.36 \text{ W / m}^2$$

For cooling from 1 150 °C:

$$Nu_{\eta} = 80,706$$

$$h = 26.475 \text{ W / m}^2$$

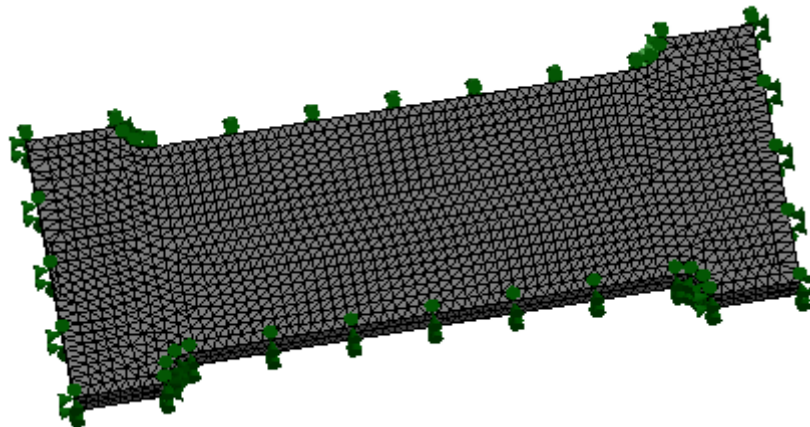
Once the individual heat transfer coefficient is known, the corresponding simulations are carried out.

The cooling rate can be defined as the variation of the temperature in time during the cooling process of the heated specimens. This variation can be obtained experimentally by measuring the value of the temperature at different times. This requires sensors that allow different measurements to be made. Another way to determine the relationship between temperature and time can be the numerical simulation of the process. These simulations will serve to obtain a curve that relates the two aforementioned parameters for the cooling of the specimen in each thermal treatment carried out. From each cooling curve an equation is obtained that relates the temperature T and the time t. The cooling velocity can be obtained by deriving (10) and determining the limit for the instant that it is desired to know  $v_e$  (the beginning of cooling) (10a); that is:

$$v_e = \frac{\delta T}{\delta t} \quad (10)$$

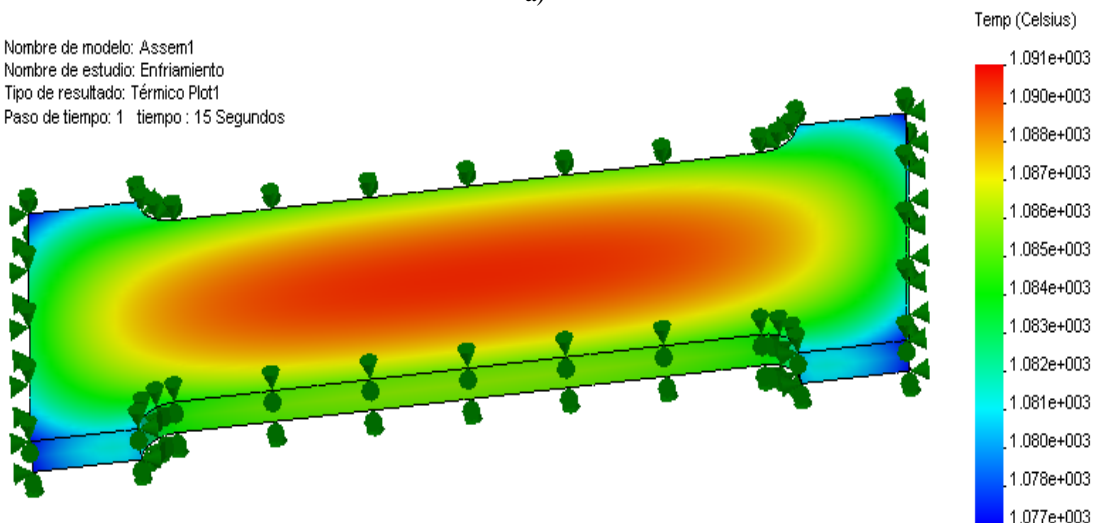
$$v_e = \left| \lim_{\Delta t \rightarrow 0} \frac{\Delta T}{\Delta t} \right| \quad (10a)$$

To perform the simulations, a solid mesh was selected, with an element size of 1,989 mm and a tolerance of 0,000099 mm. The type of study that is carried out is thermal in transitory regime. In Fig. 7 a) the test piece with the meshing carried out is shown. Each finite element has one degree of freedom per node, which corresponds to the temperature in it.

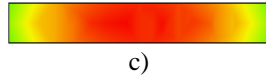


a)

Nombre de modelo: Assem1  
 Nombre de estudio: Enfriamiento  
 Tipo de resultado: Térmico Plot1  
 Paso de tiempo: 1 tiempo : 15 Segundos



b)



c)

**Figure 7.** a) Solid mesh to perform the thermal studies of the cooling speed. b) Distribution of the isotherms 15 seconds after the beginning of the cooling of the heated specimen at 1 150 °C. c) Distribution of the isotherms 15 seconds after the start of cooling in the cross section of the test piece heated to 1 150 °C.

**Fig. 7.b)** and c) show a scheme of the distribution of the isotherms 15 seconds after beginning to perform cooling for the test specimen treated at 1150 °C. As it is observed, the hottest zone corresponds to the center of the specimen.

On the other hand, Fig. 8 shows a comparison of the cooling curves of the three treatments carried out. The different curves are drawn for the node 573 located in the center of the specimen.

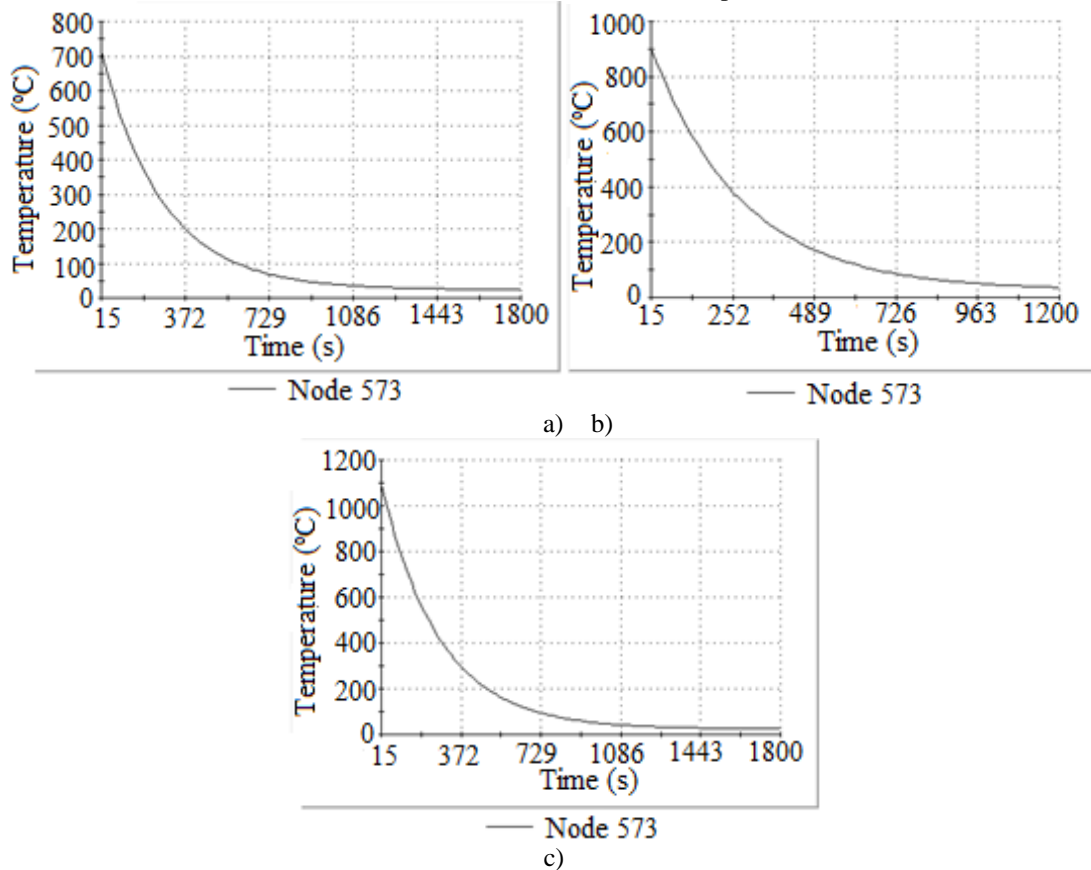


**Figure 8.** Cooling curves of node 573 a) test piece heated to 750 °C. b) test piece heated to 950 °C. c) test piece heated to 1150 °C.

The equations and the cooling speeds obtained from the previous curves are the following (11 to 13):

For cooling from 750 °C:

$$T = 0,000006t^6 - 0,0007t^5 + 0,0372t^4 - 1,0282t^3 + 16,903t^2 - 161,9t + 750,61 \quad (11)$$

$$v_c = 161,9 \text{ } ^\circ\text{C}/\text{min}$$

Para el enfriamiento a partir de 950 °C:

$$T = 0,000008t^6 - 0,0009t^5 + 0,0465t^4 - 1,2907t^3 + 21,3t^2 - 204,91t + 950,81 \quad (12)$$

$$v_c = 204,91 \text{ } ^\circ\text{C}/\text{min}$$

Para el enfriamiento a partir de 1 150 °C:

$$T = 0,00005t^6 - 0,0012t^5 + 0,0583t^4 - 1,6061t^3 + 26,306t^2 - 251,38t + 1151 \quad (13)$$

$$v_c = 251,38 \text{ } ^\circ\text{C}/\text{min}$$

#### IV. DISCUSSION

The microhardness chains made to a welded joint and to the heat treated specimens show that those corresponding to the first tend towards the mean values of the second ones. In this way in Fig. 4 it was observed that towards the part that corresponds to the overheating zone within the HAZ, the chains of microhardness tended toward the line of the specimen treated at 1150 °C, which is precisely the one with which intended to

simulate the behavior of this zone. Similar behavior was observed in other parts of the welded joint, which would correspond to the annealing and first transformation zones respectively.

Fig. 6 shows similarities between the grain size of the coarse grain area simulated by thermal treatments and that formed in a welded joint. It is also possible to observe in that same figure elongated needles. These correspond to Widmanstaetten structures. This is a structure that is characterized by having great fragility, with needles that follow several directions. It usually occurs in the molten zone, although it also occurs in the HAZ. It causes a small impact resistance, that is, it increases the brittleness of the welded joint and decreases the toughness of the coarse-grained zone of the HAZ, which is generally where the fatigue failure of the welded joints occurs in most of the cases.

The similarities found in the metallographic structures shown in Figs. 5 and 6 let us say that it is possible to simulate by thermal treatments the different zones of the HAZ in a welded joint. At the same time the results of this work show once again the difference of the properties in the different areas of the HAZ. In the tensile tests carried out, it was obtained that the Modulus of elasticity of all the specimens, after being heated at different temperatures, was similar, however there are differences in the values of the yield strength and the breakage, the highest being those corresponding to the test piece heated up to 750 °C and the smaller ones in the heated samples up to 1 150 °C. Precisely in that area in the case of a welded joint, it is where the failure can occur.

The correlation coefficient in expressions (11) to (13) is equal to 1, which indicates that there is a good fit in the equations obtained. The cooling rates calculated by applying (10) in (11 to 13) show once again the differences that exist in the different zones of the HAZ. There are differences between the values of the cooling speed calculated with (10) and those found in the literature.[1]

## V. CONCLUSION

It is possible to perform the simulation by thermal treatments of the metallographic structures that are formed in the HAZ of the welded joints. The thermal treatment processes must be carefully planned and controlled to try to reproduce as faithfully as possible the structural changes that occur during the welding process, where the contribution of heat takes place in an abrupt and focused manner. Cooling also happens quickly; having an important role together with the temperature reached during the heating, in the final structure that is obtained. Although there are similarities between the metallographic structures that are formed in the HAZ and those obtained in the heated specimens to simulate the first ones, the results of the welding process cannot be fully reproduced, due to the way it is applied and then Heat is dissipated in the welded joint. The increase in the heating temperature caused the decrease in the mechanical properties of the steel studied, which once again shows the differences in the properties that exist between the different zones that make up the HAZ of the welded joints. With the simulation by means of the finite element method, equations are obtained that relate the variation of temperature over time. Applying (10) later it is possible to know the cooling speed.

## VI. Acknowledgements

Pavel Michel AlmaguerZaldivar wants to acknowledge to Ph.D. Jesús Manuel Alegre Calderón, from Universidad de Burgos, Spain due to the support to realize the mechanical test. Also to the all members of the Group of Structural Integrity of the same University.

## REFERENCES

- [1]. H., Rodríguez. *Metalurgia de la soldadura*. (Pueblo y Educación, La Habana, Cuba. 1983).
- [2]. M., Reina. *Soldadura de los aceros. Aplicaciones*. (Gráficas Lormo. 3ra edición. Madrid, España, 1994).
- [3]. P.Y., Cheng. *Influence of Residual Stress and Heat Affected Zone on Fatigue Failure of Welded Piping Joints*, doctoral diss., North Carolina State University. North Carolina State, UnitedStates, 2009.
- [4]. D. E., Cárdenas. *Caracterización del comportamiento a fractura de un acero para gasoductos mediante el ensayo miniatura de punzonado*, doctoral diss., Universidad de Oviedo. Oviedo, España. 2010.
- [5]. A.S. Aloraier, S. Joshi, J.W.H. Price y K. Alawadhi. *Material properties characterization of low carbon steel using TBW and PWHT techniques in smooth-contoured and U shape geometries*. *International Journal of Pressure Vessels and Piping*.111–112().2013. 269–278.
- [6]. J.C. Ferreira, S.M. Faragasso, L.F. Guimaraes de Souza and I. de Souza Bott. *Efeito do tratamento térmico pós-soldagem nas propriedades mecânicas e microestruturais de metal de solda de aço de extra alta resistência para utilização em equipamentos de ancoragem*. *Soldagem&Inspeção*. 18(2). 2013. 138-148.
- [7]. X. Yue, X. Feng and J. C. Lippold. *Strength increase in the coarse-grained heat-affected zone of a high-strength, blast-resistant steel after post-weld heat treatment*. *Materials Science & Engineering A*. 585(), 2013. 149–154.
- [8]. Y. Liu, L. Qing Yang, B. Feng, Sh. Wu Bai and X. Chang. *Physical Simulation on Microstructure and Properties for Weld HAZ of X100 Pipeline Steel*. *Materials Science Forum*. 762(), 2013 556-561.
- [9]. A. Scotti, H. Li and R. M. Miranda. *A Round-Robin Test with Thermal Simulation of the Welding HAZ to draw CCT diagrams: a need for harmonized procedures and microconstituent terminologies*. *Soldag. Insp. São Paulo*, 19(03), 2014, 279-290.
- [10]. X. Kong, G. Huang, K. Fu, F. Liu, M. Huang y Y. Zhang. *“Effect of Pipe Body Alloy on Weldability of X80 Steel”*. *HSLA Steels 2015, Microalloying 2015 & Offshore Engineering Steels 2015*. Springer, Cham. pp. 467-474 November, 2015. Print ISBN 978-3-319-48614-7. Online ISBN 978-3-319-48767-0. DOI: 10.1007/978-3-319-48767-0\_55.

- [11]. J. Kulhánek, P. Tomčík, R. Trojan, M. Juránek y P. Klaus. Experimental modeling of weld thermal cycle of the heat affected zone (HAZ). *Metalurgija*, 55(4), 2016. 733-736.
- [12]. M. St. Węglowski, M. Zeman and A. Grocholewski. Effect of welding thermal cycles on microstructure and mechanical properties of simulated heat affected zone for a weldox 1300 ultra-high strength alloy steel. *Arch. Metall. Mater.*, 61(1), 2016. 127–132.
- [13]. J. Moon, J. J. Lee, Ch.-H. Lee, J.-Y. Park, T.-H. Lee, K.-M. Cho, H.-U. Hong and H. Chan Kim. Reheating cracking susceptibility in the weld heat-affected zone of a reduced activation ferritic-martensitic steel for fusion reactors. *Fusion Engineering and Design*, 124(), 2017, 1038-1041.
- [14]. M. Almaguer-Zaldivar, R. Estrada-Cingualbres. Experimental and numerical evaluation of the fatigue behaviour in a welded joint. *IOP Conf. Series: Materials Science and Engineering* 65, 2014.
- [15]. M. Almaguer-Zaldivar and R. Estrada-Cingualbres. Evaluación del comportamiento a fatiga de una unión soldada a tope de acero AISI 1015. *Ingeniería Mecánica*, 18(1), 2015, 31-41.
- [16]. MatWeb, Your Source for Materials Information. <http://www.matweb.com>, Viewed on February, 20, 2018.
- [17]. Oficina Nacional de Normalización. NC 04-01. Ensayos de tracción de metales. Cuba. 1966.
- [18]. A. P., Guliáev. *Metalografía*. Tomo 1. (Mir., Moscú, URSS, 1978).
- [19]. ASTM International. Norma ASTM E 384–99. Standard Test Method for Microindentation Hardness of Materials. 2000. Estados Unidos.
- [20]. E. A., Kranoschiokov, *Problemas de termotransferencia*. (Mir, Moscú, URSS. 1977).

Pavel-Michel Almaguer-Zaldivar" Simulation of the metallographic structures in the heat affected zone of a welded joint" *International Journal of Engineering Science Invention (IJESI)*, Vol. 08, No. 06, 2019, PP23-35